
Towards transparent ANN wind turbine power curve models

Simon Letzgus

Machine Learning Group
Technische Universität Berlin
Berlin, 10587, Germany
simon.letzgus@tu-berlin.de

Abstract

Accurate wind turbine power curve models, which translate ambient conditions into turbine power output, are crucial for wind energy to scale and fulfil its proposed role in the global energy transition. Machine learning methods, in particular deep neural networks (DNNs), have shown significant advantages over parametric, physics-informed power curve modelling approaches. Nevertheless, they are often criticised as opaque black boxes with no physical understanding of the system they model, which hinders their application in practice. We apply Shapley values, a popular explainable artificial intelligence (XAI) method, to, for the first time, uncover and validate the strategies learned by DNNs from operational wind turbine data. Our findings show that the trend towards ever larger model architectures, driven by the focus on test-set performance, can result in physically implausible model strategies, similar to the Clever Hans effect observed in classification. We, therefore, call for a more prominent role of XAI methods in model selection and additionally offer a practical strategy to use model explanations for wind turbine condition monitoring.

1 Introduction

The energy sector is responsible for the majority of global greenhouse gas emissions [1] and wind energy is to play a major role in its decarbonisation [2]. Accurate wind turbine power curve models, which translate ambient conditions into turbine power output, are important enablers for this transition. Coupled with meteorological forecasts, they are key for energy yield prediction [3, 4] and thereby help to increase the share of wind energy while keeping the electricity grid stable, despite the intermittent nature of the wind resource. Moreover, they can be successfully used for wind turbine condition monitoring [5, 6], which reduces turbine downtime and directly increases the amount of renewable energy in the electricity mix.

Power curve modelling has received plenty of attention (see [7] for a comprehensive review). While early approaches have mainly focused on parametric models based on physical considerations (e.g. [5]), vanilla DNNs have become the state-of-the-art today [8, 6, 9, 3, 4]. On the other hand, DNNs come with some fundamental challenges related to their lack of causal or physical understanding of the data-generating process, and the difficulty to convey their implicit strategy to the user.

Indeed, the wind energy community has often called for more transparent deep learning models to increase trust and obtain actionable results (e.g. [7, 10, 11]). In this contribution, we address these concerns by applying a popular method from the XAI domain, Shapley values, to both, data-driven and physics-informed models. This enables us to understand the strategies learned by DNNs and validate them against physical intuition. Additionally, we show how Shapley attributions of models with physically plausible strategies can be used for improved wind turbine condition monitoring.

2 XAI method, Data and Models

2.1 Shapley attributions for power curve models

To analyse the implicit strategy of power curve models we use *Shapley values* [12, 13, 14]. The approach determines the contribution of a feature by removing it and observing the averaged difference with and without the feature, over all permutations:

$$A_i = \sum_{S|i \notin S} \alpha_S \cdot [f(x_{S \cup \{i\}}) - f(x_S)]$$

where x is a data point composed of N features. $\sum_{S|i \notin S}$ is a sum over all subsets of features that do not contain feature i , and x_S the data point x where only features in S have been retained (the other features have been set to zero or the value of some meaningful reference point \tilde{x}). The normalisation constant $\alpha_S = |\mathcal{S}|!(N - |\mathcal{S}| - 1)/N!$ ensures conservative explanations, meaning that $\sum A_i = f(x)$.

A remaining challenge and active field of research is how to evaluate and present XAI attributions to domain experts for maximal benefit [15, 16]. Here, we make use of the model-agnostic nature of Shapley values, which enables their application to both physical and data-driven models. Consequently, we can use the correlation coefficient between attributions to evaluate to what extent the data-driven models follow physically reasonable strategies. Moreover, we visualise attribution distributions conditioned on the measured wind speed ($P(A_i|v_w)$). This results in curves with a high resemblance to the way power curves are typically displayed and therefore facilitates contextualisation and interpretation by domain experts (compare Figure 2).

2.2 Data & models

We use operational data from the Supervisory Control and Data Acquisition (SCADA) system of two 2 MW wind turbines and a meteorological met-mast, all located within the same site. The data set is openly accessible ¹. The data utilised spans over a whole year of operation and temporal resolution is the SCADA-typical 10min averaged sensor values. Our pre-processing pipeline includes a set of basic filters, to ensure we capture normal operation behaviour (for details see Appendix A). Overall, this results in roughly 30.000 data points per turbine, which are then randomly shuffled and divided into train, validation and test sets by a ratio of 60/20/20.

When modelling wind turbine power output, there is some choice regarding the input parameters. Here, we limit ourselves to three variables: **wind speed** (v_w), **air density** (ρ) and **turbulence intensity** (TI). Focusing on these most important environmental impact factors [17] limits the complexity of the physics-informed model and facilitates the evaluation of the learned strategies. For each turbine we fit a physics-informed, parametric model and several data-driven models:

Physics-informed models: For the physics-informed baseline power curve model, we follow the widely adopted international standard IEC 61400-12-1 [17]. It describes in detail the industry standard for power-curve modelling, including correction methods for air density and turbulence intensity. For more details, please refer to Appendix B.

Data-driven models: we train two fully connected artificial neural network (ANN) architectures (hidden layers/neurons per layer) with ReLU-activations: ANN small (3/20) and ANN large (5/100). This enables us to analyse the impact of model size on the learned strategies. Both models are trained using ADAM [18] with a mild regularisation ($\lambda = 0.01$), a learning rate of 0.01 and early stopping after 25 epochs. We trained 25 models with different random initialisations and chose the ten models with the best test-set error for our evaluation.

Figure 1 (left) shows that the ANNs consistently outperform the physical model and that the large model shows clear improvements over the small ANNs. This is in line with previous research ([6, 9, 3, 4]). Note, that the displayed errors are normalised by the RMSEs of the physical models (for results in absolute terms see Appendix C). They amount to 43.39 kW and 36.96 kW for Turbines A and B (T_A and T_B), respectively. The difference is surprisingly large and suggests, that the recorded data of T_A contains traces of effects beyond the considered physical phenomena. These can originate, for example, from the specific aerodynamic conditions due to the turbine’s location within the farm.

¹<https://opendata.edp.com>

3 Experiments & Results

In the first section (3.1), we measure how close the learned DNN strategies are to those of the respective physical models. Once the strategy of a model is validated, its attributions can be used to gain further insights, which we explore in section 3.2.

3.1 How much physics did the models learn?

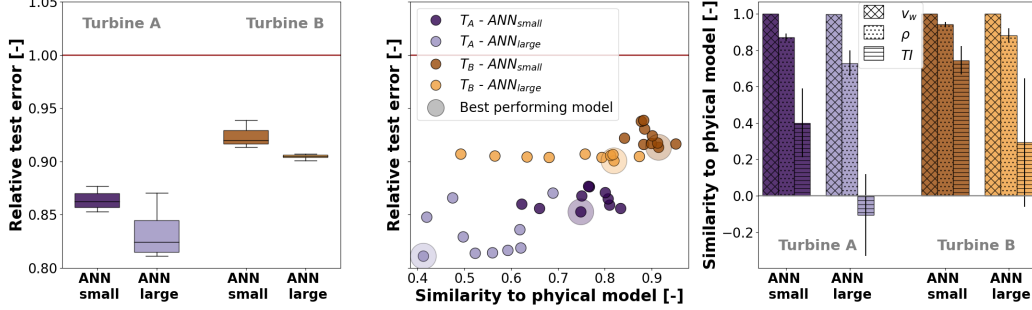


Figure 1: Comparison of model performance (left) and strategy (centre, right) for all architectures, initialisations and turbines. The left plot shows the distribution of ANN test errors relative to the physical model errors. The other two plots show the mean correlation coefficient between attributions of ANNs and physical models, for each initialisation (centre) and for each input feature (right).

Figure 1 shows the similarity of ANN strategies with the physical models per initialisation (centre) and input feature (right) across both model architectures and turbines. Several interesting observations can be made:

Impact of model initialisation: it becomes clear, that model initialisation can not only have a profound impact on model performance but also on the adapted model strategy (Figure 1, centre). Interestingly, it is never the best performing model that shows the highest agreement with physical model strategies and a more physical model with almost identical test-set performance can be found.

Impact of model architectures: the results show that model architecture has a much more significant and systematic impact on model strategies than initialisation. The large DNNs consistently outperform the small ones in terms of RMSE but exhibit much lower agreement with physical model strategies.

Impact of data: when comparing the strategies of models trained on data from T_A and T_B , we can observe that the models for T_B show a much higher overall agreement with physics-informed model strategies. In the light of the respective performance of the physical models (compare Appendix C), this seems reasonable.

Strategies by input parameters: all model strategies show a clear ranking, both in mean and variance, that coincides with the physical relevance of the respective input parameter (Figure 1, right). The influence of wind speed (v_w), the by far most crucial input, is captured very accurately across models and turbines, followed by the reasonably well-captured influence of air density (ρ). For turbulence intensity (TI) the models seem to have difficulties and partially fail to account for its influence in a physics-informed manner.

In Figure 2 we visualise the strategies for two of the best-performing ANNs (compare Figure 1, centre) by input parameter to get a better quantitative understanding of the model strategies. While model $T_B - ANN_{small}$ (brown) captures the relationships in almost a textbook manner, model $T_A - ANN_{large}$ (mauve) fails in almost every aspect. All ANNs overestimate the influence of ρ compared to the physical baseline (centre plot), however, this effect is more pronounced for the large models. Whether they are able to capture additional effects related to seasonality or this is caused only by spurious correlations remains up to speculation. In terms of TI (right plot), models for T_B follow the physical baseline reasonably well, especially in contrast to model $T_A - ANN_{large}$.

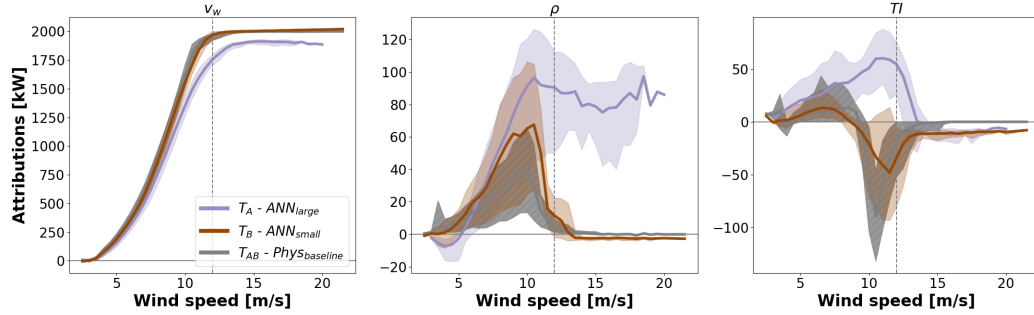


Figure 2: Conditional distributions of attributions (mean as lines, range shaded) for physical model (grey, hatched) and two selected ANNs (colourful). The curves show the wide range of adapted strategies and exemplify the findings presented in Figure 1, right, on for individual models.

3.2 Explaining potential root-causes for turbine underperformance

Once a data-driven model’s strategy is considered physically valid, its attributions can also be used in terms of absolute magnitudes, if the XAI method is conservative [19]. Here, we focus on a prominent application of power curve models, the detection of turbine underperformance [5, 20, 6, 21, 22]. A major drawback of the commonly utilised reconstruction-based anomaly detection approaches is, that they don’t allow for an indication of potential root causes. By including additional technical parameters into the power curve model, such as the blade-pitch angle or a yaw-misalignment feature, and carefully choosing the reference point \tilde{x} , the attributions can directly hint at or exclude potential root causes of underperformance, a decisive advantage in SCADA based monitoring. An example can be found in Appendix D.

4 Conclusions

So far, the trend towards deeper and wider ANN architectures in data-driven power curve modelling was justified based on superior test-set performance. The results from this contribution suggest, that this might be on the cost of physically reasonable model strategies. The findings show similarities to the famous Clever-Hans effect in classification [23]. Whether the deviation from physical intuition can have similarly harmful implications, should be the subject of further research.

In any case, we recommend including the analysis of model strategies in the model selection process since often physically more plausible models were obtained with only minor performance losses. Overall, it has to be considered whether a focus on smaller models that better capture physical phenomena would be the right way forward, especially given the demonstrated value of such models in the condition monitoring context. Another benefit of smaller architectures would be the reduced carbon footprint when training individual models for each turbine of a large fleet.

With this work, we have laid the foundation for transparent data-driven wind turbine power curve models. We hope that the insights will help practitioners to more effectively utilise their DNN models and turbines; along with the related positive implications for the global energy transition.

References

- [1] Hannah Ritchie, Max Roser, and Pablo Rosado. Co₂ and greenhouse gas emissions. *Our World in Data*, 2020. <https://ourworldindata.org/co2-and-other-greenhouse-gas-emissions>.
- [2] Global Wind Energy Council. Gwec| global wind report 2022. *Global Wind Energy Council: Brussels, Belgium*, 2022.
- [3] Mike Optis and Jordan Perr-Sauer. The importance of atmospheric turbulence and stability in machine-learning models of wind farm power production. *Renewable and Sustainable Energy Reviews*, 112:27–41, 2019.

- [4] Jordan Nielson, Kiran Bhaganagar, Rajitha Meka, and Adel Alaeddini. Using atmospheric inputs for artificial neural networks to improve wind turbine power prediction. *Energy*, 190:116273, 2020.
- [5] Andrew Kusiak, Haiyang Zheng, and Zhe Song. On-line monitoring of power curves. *Renewable Energy*, 34(6):1487–1493, 2009.
- [6] Meik Schlechtingen, Ilmar Ferreira Santos, and Sofiane Achiche. Using data-mining approaches for wind turbine power curve monitoring: A comparative study. *IEEE Transactions on Sustainable Energy*, 4(3):671–679, 2013.
- [7] Vaishali Sohoni, SC Gupta, and RK Nema. A critical review on wind turbine power curve modelling techniques and their applications in wind based energy systems. *Journal of Energy*, 2016, 2016.
- [8] Kittipong Methaprayoon, Chitra Yingvivatanapong, Wei-Jen Lee, and James R. Liao. An integration of ann wind power estimation into unit commitment considering the forecasting uncertainty. *IEEE Transactions on Industry Applications*, 43(6):1441–1448, 2007.
- [9] Francis Pelletier, Christian Masson, and Antoine Tahan. Wind turbine power curve modelling using artificial neural network. *Renewable Energy*, 89:207–214, 2016.
- [10] Guilherme A Barreto, Igor S Brasil, and Luis Gustavo M Souza. Revisiting the modeling of wind turbine power curves using neural networks and fuzzy models: an application-oriented evaluation. *Energy Systems*, pages 1–28, 2021.
- [11] Joyjit Chatterjee and Nina Dethlefs. Facilitating a smoother transition to renewable energy with ai. *Patterns*, 3(6):100528, 2022.
- [12] L. S. Shapley. *A Value for n-Person Games*, pages 307–318. Princeton University Press, 1953.
- [13] Erik Strumbelj and Igor Kononenko. An efficient explanation of individual classifications using game theory. *J. Mach. Learn. Res.*, 11:1–18, 2010.
- [14] Scott M. Lundberg and Su-In Lee. A unified approach to interpreting model predictions. In *NIPS*, pages 4765–4774, 2017.
- [15] Andreas Holzinger, Georg Langs, Helmut Denk, Kurt Zatloukal, and Heimo Müller. Causability and explainability of artificial intelligence in medicine. *Wiley Interdisciplinary Reviews: Data Mining and Knowledge Discovery*, 9(4):e1312, 2019.
- [16] Wojciech Samek, Grégoire Montavon, Sebastian Lapuschkin, Christopher J. Anders, and Klaus-Robert Müller. Explaining deep neural networks and beyond: A review of methods and applications. *Proceedings of the IEEE*, 109(3):247–278, 2021.
- [17] Wind energy generation systems – part 12-1: Power performance measurements of electricity producing wind turbines. Standard IEC 61400-12-1, International Electrotechnical Commission, Geneva, Switzerland, 2017.
- [18] Diederik P Kingma and Jimmy Ba. Adam: A method for stochastic optimization. *arXiv preprint arXiv:1412.6980*, 2014.
- [19] Simon Letzgus, Patrick Wagner, Jonas Lederer, Wojciech Samek, Klaus-Robert Müller, and Grégoire Montavon. Toward explainable artificial intelligence for regression models: A methodological perspective. *IEEE Signal Processing Magazine*, 39(4):40–58, 2022.
- [20] Meik Schlechtingen, Ilmar Ferreira Santos, and Sofiane Achiche. Wind turbine condition monitoring based on scada data using normal behavior models. part 1: System description. *Applied Soft Computing*, 13(1):259–270, 2013.
- [21] Shane Butler, John Ringwood, and Frank O’Connor. Exploiting scada system data for wind turbine performance monitoring. In *2013 Conference on Control and Fault-Tolerant Systems (SysTol)*, pages 389–394, 2013.
- [22] Joon-Young Park, Jae-Kyung Lee, Ki-Yong Oh, and Jun-Shin Lee. Development of a novel power curve monitoring method for wind turbines and its field tests. *IEEE Transactions on Energy Conversion*, 29(1):119–128, 2014.
- [23] Sebastian Lapuschkin, Stephan Wäldchen, Alexander Binder, Grégoire Montavon, Wojciech Samek, and Klaus-Robert Müller. Unmasking clever hans predictors and assessing what machines really learn. *Nature Communications*, 10:1096, 2019.
- [24] A Albers. Turbulence and shear normalisation of wind turbine power curve. *development*, 3:4, 1994.

A Data pre-processing

Data pre-processing for the validation of ANN strategies with respect to physical intuition (section 3.1) consists of three consecutive filtering steps:

1. Non-operational periods: turbine power output < 0 kW
2. Abnormal operation points 1: deviations from manufacturer power curves > 250 kW
3. Abnormal operation points 2: deviations from the norm-pitch-curve $> \pm 1^\circ$

When explaining underperformance events (section 3.2 and Appendix D), we relax the limit in filtering step 2 to 500 kW since we want to capture large underperformance events and do not conduct filtering step 3, since we explicitly include a blade-pitch angle feature.

B Physics-informed baseline model

To faithfully evaluate the ANN explanations, we create a physics-informed benchmark by applying Shapley values to a physical model. For each turbine, we calculate the binned power curve and apply air density, as well as TI corrections following the IEC standard [17]. Air density correction is straightforward as described in equation 1 using the site's mean air density over the measurements period (ρ_0). For the TI correction we calculate the zero TI-reference power curve ($P_{TI=0}(v)$), which we then correct using equation 2 with the respective wind speed distribution ($p(v)$). More details can be found in [24] and Appendix M of IEC 61400-12 [17].

$$V_n = V_{free} \left(\frac{\rho_{10 \min}}{\rho_0} \right)^{1/3} \quad (1)$$

$$\overline{P_{sim}(v)} = \int_{v=0}^{\infty} P_{TI=0}(v) \cdot p(v) dv \quad (2)$$

All required parameterisations for the physics-informed model (binned power curve, average air density and zero TI-reference power curve) are calculated using the training data set. Performance evaluation and explanations are calculated for the test set.

C Overview model performance

Table 1: Overview of models and their performance

Model	Architecture	Turbine A		Turbine B	
	layers x neurons	RMSE [kW]		RMSE [kW]	
$Phys_{baseline}$	-	43.39		36.96	
ANN_{small}	3x20	37.48 ± 0.37		34.13 ± 0.34	
ANN_{large}	5x100	34.12 ± 0.96		33.45 ± 0.07	

D Explaining performance deviations

For explaining underperformance events, we include two additional technical input variables, blade-pitch angle (λ_{pitch}) and a yaw-misalignment feature (Yaw_{mis}). Also, we relax the data filtering (compare Appendix A) to allow for underperformance events in the data. We train a model of architecture ANN_{small} on data from (T_B).

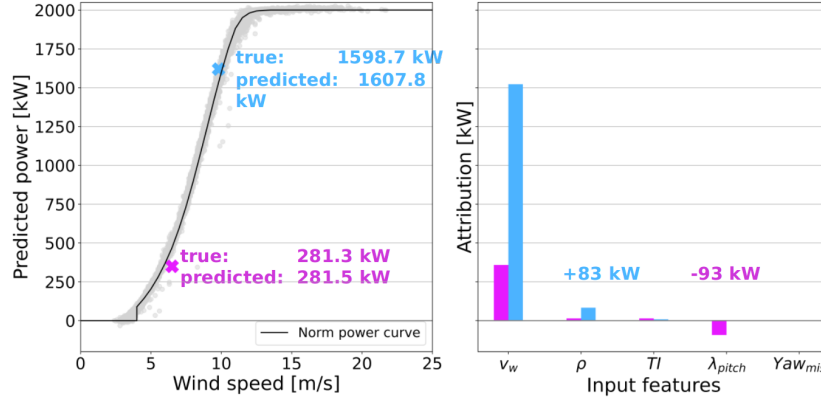


Figure 3: Attributions generated for two selected instances. On the left, the selected data points are marked relative to the turbine’s standard power curve, given by the operator. The colour code applies to the right plot, where the model output for each of the data points is attributed to the respective input features.

Now, we can analyse the attributions for single 10min instances. Figure 3 shows the decomposition of the function value $f(x)$ into the attributions A_i per input feature i for two of these instances. For the blue instance, we can see that the model correctly captures a relative over-performance of the turbine with respect to the power curve given by the manufacturer. The attributions indicate that this is due to favourable ambient conditions, in particular, a high air density ρ . For the pink instance, we can see that the model correctly captures the relative underperformance of the turbine with respect to the power curve given by the manufacturer. The attributions indicate, however, that this is not due to unfavourable ambient conditions but instead one of the technical features is clearly highlighted. The blade-pitch angle is an actively controlled parameter and its deviation from the norm might be problematic. This information can be crucial for condition monitoring applications and maintenance personnel can be sent into the field with much more detailed instructions.